Nano-Scaled Ordering of Hyperbranched and Star-Hyperbranched Polymers

Koji Ishizu, Koichiro Ochi, Taiichi Furukawa

Department of Organic Materials and Macromolecules, International Research Center of Macromolecular Science, Tokyo Institute of Technology, 2–12-1-H-133, Ookayama, Meguro-ku, Tokyo 152-8552, Japan

Received 30 October 2004; accepted 31 July 2005
DOI 10.1002/app.23559
Published online in Wiley InterScience (www.interscience.wiley.com).

ABSTRACT: Hyperbranched polystyrenes (HPS) were prepared by living radical polymerization of 4-vinylbenzyl *N,N*-diethyldithiocarbamate (VBDC) as an inimer under UV irradiation. These HPS exhibited large amounts of photofunctional diethyldithiocarbamate (DC) groups on their outside surfaces. We derived star-HPS (SHPS) by grafting from such HPS macroinitiator with methyl methacrylate (MMA) or ethyl methacrylate (EMA). The ratios of radius of gyration to hydrodynamic radius R_g/R_h for HPS and SHPS in tetrahydrofuran (THF) were in the range of 0.74–0.90 and 1.05–1.12, respectively. HPS and SHPS behaved in a good solvent as hard and soft spheres, respectively. We demonstrated the structural ordering of both branched polymers in THF through small-angle X-ray scattering (SAXS), by varying the polymer concentration. As a result, HPS and SHPS formed face-centered-cubic (fcc) and body-centered-cubic (bcc) structures, respectively, near the overlap threshold (C^*).
 J Appl Polym Sci 100: 3340–3345, 2006

Key words: hyperbranched polymer; star-hyperbranched copolymer; nano-scaled ordering; SAXS

INTRODUCTION

The properties of stars, hyperbranched polymers, and dendrimers have been shown to be very different from those of linear polymers. For example, the lack of entanglements results in a lower viscosity. The large extent of end functional groups causes higher solubility in various solvents for hyperbranched polymers and dendrimers compared with linear structure, at a given molecular weight.[1–3] On the other hand, star polymers are characterized as the simplest structure of branched species, where all chains are connected to a core of small molecular mass. Stars with multiarms (the critical number of arms is estimated to be of order 10^2) are expected to form a crystalline array near the overlap threshold (C^*) by Witten et al.[4] Recently, we studied structural ordering of polyisoprene (PI)[5] and peripherally charged poly(ethylene oxide) (PEO) stars[6] by small-angle X-ray scattering (SAXS). PI stars (arm number $f > 91$) formed a body-centered-cubic (bcc) structure near the C^*. On the other hand, peripherally charged PEO stars ($f > 37$) formed a lattice of bcc even below C^*. The results indicated that ionization (electric double layer) of PEO stars resulted in interparticle interactions giving rise to ordering. This structure changed to the mixed lattice of bcc and a face-centered-cubic (fcc) for both stars, with increasing the polymer concentration. Consequently, we carried out the double-logarithmic plot of the nearest-neighbor distance of the spheres (D_0) as a function of polymer concentration. It was found that the measured D_0 was proportional to the -0.32th power of the polymer concentration and fitted well with the $-1/3$ power expected for homogeneous system. This fact indicated that the spherical particles led to isotropic shrinkage with increasing the polymer concentration. Watzlawek et al. also showed a phase diagram for star polymers with regions of fcc and bcc order, in terms of the arm numbers.[7] Such structural ordering of stars was very similar to hierarchical structure transition of the cubic lattices observed on the core-shell microspheres[8,9] and $(AB)_n$ stars.[10] That is to say, these multicomponent branched copolymers formed a bcc structure near the C^*. This structure changed to the mixed lattice of bcc and fcc with increasing the polymer concentration. In the bulk, these particles were packed in the lattice of an fcc.

Recent experimental investigations of the internal structure of dendritic macromolecules with small-angle neutron scattering (SANS) and SAXS methods showed that the dendrimers in solution seemed to be like ball-shaped monodisperse particles with a uniform inner density distribution, and the averaged volume density was close to their bulk density.[11–16] There are also a few reports concerning the structural ordering of hyperbranched polymers[17,18] and dendrimers with different chemical structure.[13,19] Although these studies showed the appearance of ordering, the structural analysis of cubic lattices was not performed in detail.

Correspondence to: K. Ishizu (kishizu@polymer.titech.ac.jp).

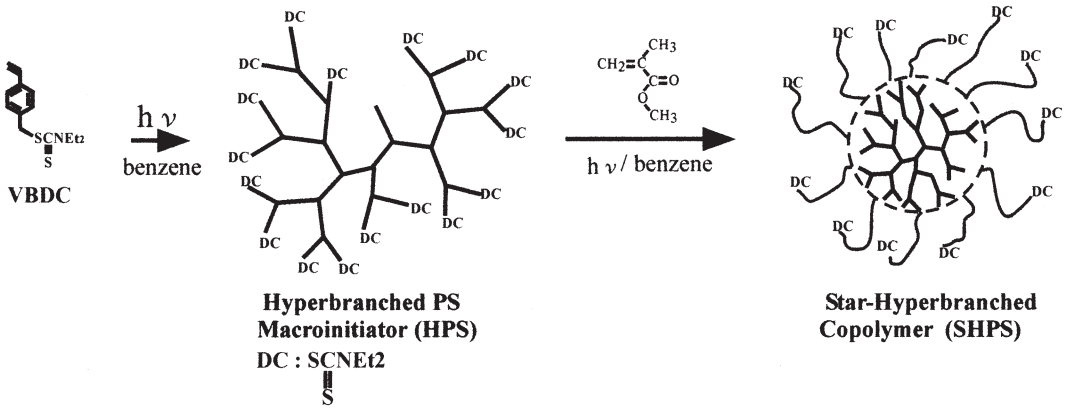

Scheme 1

More recently, we presented a novel route to hyperbranched polystyrene (HPS)[20] and hyperbranched poly(ethyl methacrylate) (HPEMA)[21] from 4-vinylbenzyl *N,N*-diethyl-dithiocarbamate (VBDC) and 2-(*N,N*-diethyldithiocarbamyl)ethyl methacrylate (DTCM), respectively, as the inimer by one-pot photopolymerization. For example, photolysis of VBDC leads to the initiating benzyl radical with inactive diethyldithiocarbamate (DC) radical. This radical mechanism is very similar to the alkoxyamine-initiated living radical polymerization system, details of which were published by Moad and Rizzardo.[22] Such hyperbranched polymers formed a single molecule in solution due to a very high inner density. In fact, such hyperbranched molecules behaved as "hard sphere" in solution.[23,24] Since the hyperbranched polymer has large amounts of photofunctional DC groups on its outside surface, we could derive star-hyperbranched copolymers (SHPS) by graft photopolymerization of HPS as a macroinitiator with other vinyl monomers.[25]

In this study, HPS was prepared by living radical photopolymerization of VBDC under UV irradiation. Subsequently, we prepared SHPS by grafting from HPS macroinitiator with methyl methacrylate (MMA) or ethyl methacrylate (EMA). Both branched polymers formed single nanospherical molecule in tetrahydrofuran (THF). We also made clear the structural ordering of both branched polymers in THF through the SAXS and atomic force microscopy (AFM) measurements, by varying the polymer concentration.

EXPERIMENTAL

Materials

VBDC was synthesized by the reaction of *p*-chloromethylstyrene with DC sodium salt. Details concerning the synthesis and characterization have been given elsewhere.[20] MMA and EMA (Tokyo Kasei, Tokyo) were distilled in high vacuum. Benzene, methanol, THF, chloroform, *m*-xylene, acetonitrile, and *N,N*-tetraethylthiuram disulfide (TD; Tokyo Kasei) were used as-received.

Synthesis of HPS and SHPS

The synthetic route of HPS and SHPS is shown in Scheme 1. HPS was synthesized by photopolymerization of VBDC. The precipitation fractionation of HPS was carried out with a benzene–methanol system, because the HPS exhibited a broad molecular weight distribution. Details concerning the synthesis and purification have been given elsewhere.[20]

The SHPS was prepared by graft photopolymerization of HPS (0.1 g) with MMA or EMA (4 mL) in benzene (10 mL) in the presence of TD (0.1 g) under UV irradiation in a sealed glass ampoule under high vacuum at 30°C (250-W high-pressure mercury lamp, Ushio Denki UI 250D; UV intensity 42 mW/cm^2, irradiation distance 15 cm). After polymerization, the product was precipitated in methanol.

Dilute-solution properties of HPS and SHPS

The weight–average molecular weights (M_w) of HPS and SHPS were determined by static light scattering (SLS; Photal TMLS-6000HL Otsuka Electronics) using the Zimm mode with a He–Ne laser (λ_0 = 632.8 nm) in THF solution at 25°C. The refractive index increment of both branched polymers [$(dn/dc)_{HPS}$ = 0.181 and $(dn/dc)_{SHPS}$ = 0.101–0.081 mL/g; each value for SHPS samples is listed in Table II as described later] was determined by a refractometer in THF. The molecular weight distributions (M_w/M_n) of both branched polymers were determined by gel permeation chromatography (GPC; Tosoh high-speed liquid chromatograph HLC-8020) using polystyrene (PS) standard samples in THF as the eluent at 38°C, two TSK gel columns, GMH_{XL} [excluded-limit molecular weight (M_{EL} = 4 × 10^8)] and $G2000H_{HL}$ (M_{EL} = 1 × 10^4), in series and at a flow rate of 1.0 mL/min.

TABLE I
Solution Properties of Hyperbranched Polystyrenes

Exp. no.	M_w[a] (10^{-4})	M_w/M_n[b]	R_h[c] (nm)	R_g[d] (nm)	R_g/R_h
HPS1	7.4	1.82	4.1	3.7	0.90
HPS2	12.4	2.45	9.3	6.9	0.74

[a] Determined by SLS with Zimm mode in THF at 25°C.
[b] Determined by GPC in THF as eluent at 38°C.
[c] Determined by DLS in THF at 25°C.
[d] Determined by Guinier's plot on SAXS in THF at 25°C.

The radius of gyration (R_g) of SHPS was determined by Zimm plots. Since R_g of HPS prepared from this work was very small, the R_g was determined by SAXS using Guinier's plots as mentioned in our previous paper.[21] The hydrodymanic radii (R_h) of both branched polymers were determined using dynamic light scattering (DLS; Otsuka Electronics) with a He–Ne laser (λ_0 = 632.8 nm) in THF at 25°C. Sample solutions were filtered through membrane filters with a nominal pore of 0.2 μm just before measurements. The diffusion coefficient (D_0) was determined by the extrapolation to zero concentration of DLS data with the cumulant method in 0.40–14 mg/mL THF solution. The scattering angle was in the range of 30–150°.

^{1}H-NMR spectra were recorded on a JEOL GSX-500 NMR spectrometer in $CDCl_3$.

SAXS measurement

The SAXS intensity distribution $I(q)$ (q; scattering vector) was measured with a rotating-anode X-ray generator (Rigaku Denki Rotaflex RTP 300RC) operated at 40 kV and 100 mA. The X-ray source was monochromatized Cu Kα (λ_0 = 1.54 Å) radiation. In the measurement of the sample (THF solution), a glass capillary (ϕ = 2.0 mm, Mark-Röhchen Ltd.) was used as a holder vessel. The SAXS patterns were taken with a fine-focused X-ray source using a flat plate camera (Rigaku Denki, RU-100). The SAXS intensity profiles were plotted from the horizontal section of the SAXS patterns without considering the smearing correction.

AFM measurement

AFM photographs were recorded with a JSPM-4210 scanning probe microscope (Jeol, Tokyo) operating in the tapping mode. The measurements were performed in air using Si cantilevers with a spring constant of 0.65 N/m, a tip radius of 10 nm, and a resonance frequency of 40 kHz. The samples for tapping-mode AFM measurements were prepared by spin-casting on a rotating mica substrate at 2000 rpm of dilute solutions of HPS or SHPS in chloroform.

RESULTS AND DISCUSSION

Solution properties of HPS

The HPSs were prepared by photopolymerizations of VBDC, at varying irradiation times (4 h for HPS1 and 8 h for HPS2). The precipitation fractionation was carried out with a benzene–methanol system. Solution properties of HPS are listed in Table I. The ratio R_g/R_h is a sensitive fingerprint of the inner density profile of star molecules and polymer micelles. The values of R_g/R_h for HPS were in the range of 0.74–0.90. It is well known that R_g/R_h values for linear unperturbed polymers, and hard spheres of uniform density are 1.25–1.37[26] and 0.775,[27,28] respectively. It was concluded that the HPSs almost behaved as hard spheres in a good solvent.

Synthesis and solution properties of SHPS copolymers

Since the HPSs have large amounts of photofunctional DC groups on their outside surfaces, SHPS copolymers can be derived by grafting from the HPS macroinitiator with vinyl monomers (Scheme 1). In a preliminary experiment of graft photopolymerization of HPS with MMA, the copolymerization product led to partial gelation after 5 min of UV irradiation. This system seemed to be accompanied by disproportionation. Next, we carried out such graft copolymerization in the presence of TD. Typical GPC profile for M-SHPS11 (MMA; 4 h of irradiation) is shown in Figure 1. The GPC distribution of M-SHPS11 has a unimodal pattern and shifts to high-molecular-weight side compared to the starting HPS1 macroinitiator.

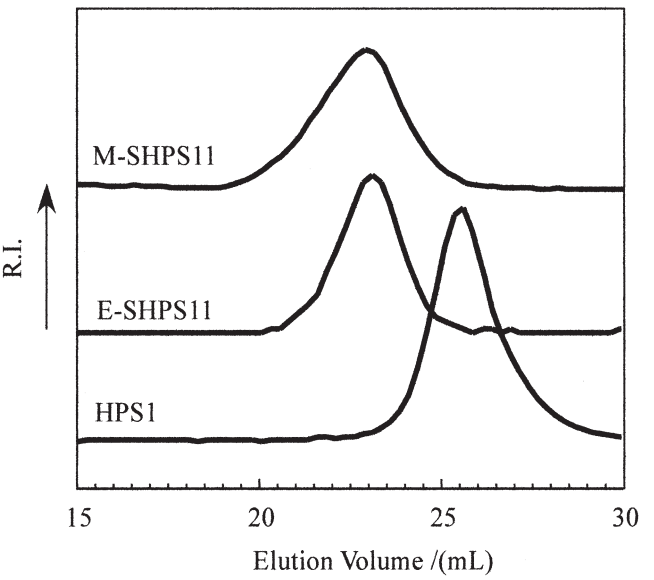

Figure 1 GPC profiles of HPS1, M-SHPS11, and E-SHPS11. GPC measurements were carried out in THF at 38°C.

TABLE II
Characteristics and Solution Properties of Star-Hyperbranched Copolymers

Exp. no.	Macroinitiator	Second monomer	$(dn/dc)_{SHPS}$ (mL/g)	M_w[a] (10^{-6})	M_w/M_n[b]	R_h[c] (nm)	R_g[a] (nm)	R_g/R_h (nm)
M-SHPS11	HPS1	MMA	0.0812	1.54	2.09	14.4	15.2	1.05
E-SHPS11	HPS1	EMA	0.1012	1.15	1.84	14.1	15.9	1.12

[a] Determined by SLS with Zimm mode in THF at 25°C.
[b] Determined by GPC in THF as eluent at 38°C.
[c] Determined by DLS in THF at 25°C.

The addition of TD may move the equilibrium balance between HPS macroinitiator and benzyl/DC radicals to the left side. The E-SHPS11 (EMA; 6 h of irradiation) provided smaller M_w than that of M-SHPS11, regardless of long irradiation time. The propagation rate of MMA was more rapid than that of EMA.

The values of M_w and R_g for SHPS copolymers were derived from a Zimm plot in THF (Table II). To discuss the geometrical anisotropy and intermolecular interaction, we determined the translational diffusion coefficient (D_0) of SHPS copolymers. In general, the mutual diffusion coefficient $D(C)$ is defined as $D(C) \equiv \Gamma_e q^{-2}{}_{\theta \to 0}$, where θ is the scattering angle. Typical angular dependence of $\Gamma_e q^{-2}$ ($qR_h < 1$) for E-SHPS11 is shown in Figure 2. In the case of spherical shapes, it is well known that the slope of line is zero. The observed data of E-SHPS11 copolymer almost fit a straight line. Therefore, it seems that SHPS copolymers take the shape of spheres in dilute solution. Figure 3 shows the relationship between translational diffusion coefficient $D(C)$ and polymer concentration C for E-SHPS11 (scattering angle 90°). Each $D(C)$ has a constant value in the range of 0–10 mg/mL polymer concentration. The M-SHPS11 showed similar results as E-SHPS11. This suggests that SHPS copolymers form a single molecule at such polymer concentration. The translational diffusion coefficient D_0 can be estimated by extrapolation of C to zero. The R_h is defined by the Stokes–Einstein equation: $R_h = kT/6\pi\eta_0 D_0$, where k, T, and η_0 indicate Boltzmann coefficient, absolute temperature, and viscosity of the solvent, respectively. The values of R_h are also listed in Table II. The values of R_g/R_h for SHPS copolymers were in the range of 1.05–1.12. As mentioned in the Introduction, star, core-shell microspheres, and $(AB)_n$ stars also possessed the similar values in dilute solution. It was concluded that the SHPS copolymers behaved as soft spheres in a good solvent.

Structural ordering of HPS and SHPS

The structural ordering of HPS and SHPS was investigated by means of SAXS in THF, by varying the polymer concentration. Below C^* [$= 3M_w/(4\pi N_A R_h{}^3)$; where N_A is the Avogadro number], both polymers remained isolated, as any arrangement in solution is expected near or above C^*. We measured first the

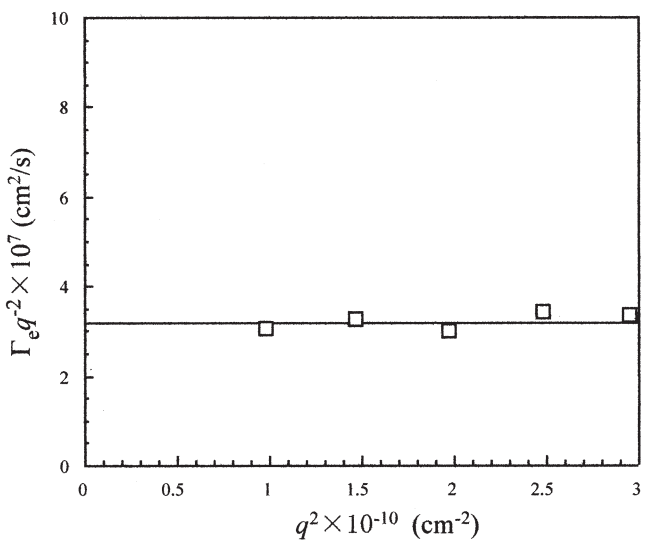

Figure 2 Angular dependence of $\Gamma_e q^{-2}$ ($qR_h < 1$) for E-SHPS11 in THF at 25°C.

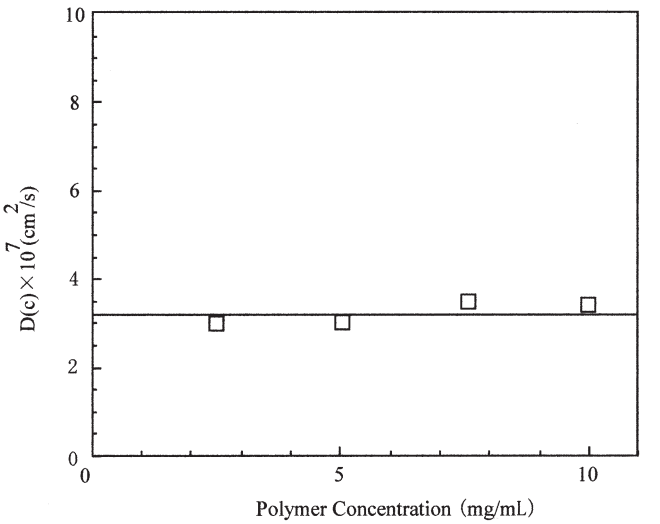

Figure 3 Relationship between translational diffusion coefficient $D(C)$ and polymer concentration C for E-SHPS11 in THF at 25°C.

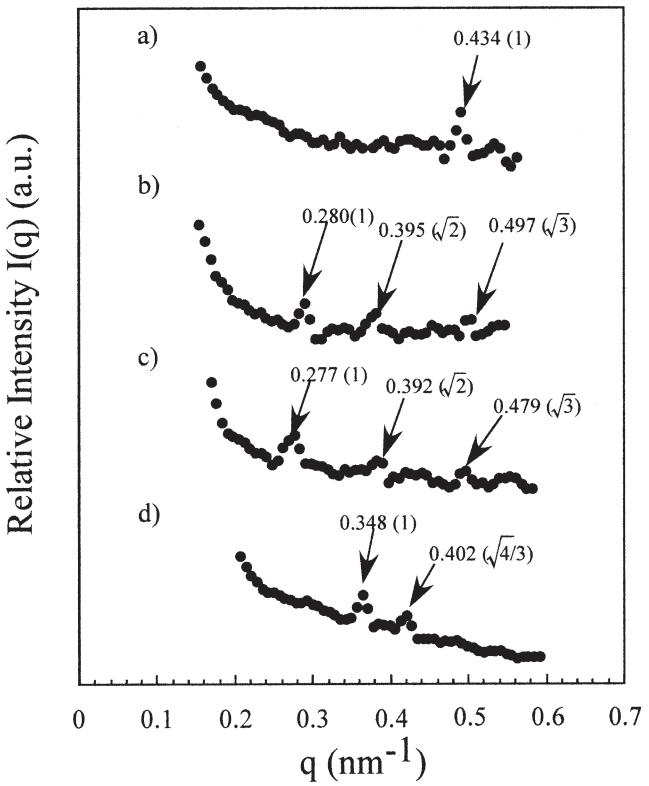

Figure 4 SAXS intensity profiles of HSP and SHPS near the *C**: (a) HPS2 in THF; (b) M-SHPS11 in THF; (c) E-SHPS11 in THF; (d) M-SHPS11 in *m*-xylene (Θ state).

SAXS intensity profiles of the HPS2 at below 2 wt % of THF solutions. These polymer concentrations were lower than the *C** (3.6 wt %). No regular scattering peaks appeared at these concentrations due to disordering. In the SAXS intensity profile at 4 wt % of polymer concentration, a single scattering peak appears as shown in Figure 4(a), where q [= $(4\pi/\lambda)\sin\theta$] (where θ is one-half the scattering angle) is the magnitude of the scattering vector. The arrow and the value in parentheses indicate the scattering maximum and interplanar spacing (d_1/d_n), respectively, calculated from the Bragg reflection. This means that the HPS2 did not take ordering structure with long range distance, though hyperbranched molecules formed some kind of cubic structure at *C**.

In the SAXS intensity profiles at the *C** for M-SHPS11 (20 wt %) and E-SHPS11 (16 wt %) [Figs. 4(b) and 4(c)], the first three peaks appear closely at the relative q positions of $1:\sqrt{2}:\sqrt{3}$, as shown in parentheses. The interplanar spacing (d_1/d_n) at the scattering angles in relative to the angle of the first maximum according to Bragg's equation is $2d\sin\theta = n\lambda$ (where λ = 1.5418 Å). In general, this packing pattern appears in the lattice of not only simple cubic but also bcc structures. As mentioned in the Introduction, the $(AB)_n$ stars, stars, and core-shell microspheres were packed in the lattice of a bcc structure near *C**. The conformation of SHPS copolymers can be regarded as similar to core-shell microspheres in solution. It is reasonable that these values correspond to the packing pattern of (110), (200), and (211) planes in a bcc structure.

TABLE III
Physical Values on Spatial Packing of Cubic Lattices for HPS and SHPS in THF Solution

Code	q_1[a] (nm^{-1})	d_1[b] (nm)	D_s[c] (nm)
HPS2	0.434	14.47	17.7
M-SHPS11	0.291	21.58	26.4
E-SHPS11	0.277	22.67	27.8

[a] Calculated by $q = 4\pi \sin\theta\lambda$.
[b] Calculated by $d_1 = 2\pi q_1$.
[c] Determined by $D_s = [(3/2)]d$.

We consider spatial packing of the cubic lattice in solution. The measured Bragg spacing d_1 is related to the nearest-neighbor distance of the spheres D_S as $D_S = [\sqrt{(3/2)}]d_1$ for bcc and fcc.

Table III lists the physical values on spatial packing of the cubic lattice for HPS and SHPS. Each value of D_S is almost identical to the corresponding hydrodynamic diameters ($2R_h$; Tables I and II).

We determined hydrodynamic diameter D_h of M-SHPS11 by means of DLS in acetonitrile or *m*-xylene as a parameter of temperature (Fig. 5). The Θ temperature of poly(methyl methacrylate) (PMMA) was 24°C in *m*-xylene.[29] The M-SHPS11 copolymer shows almost the same value of D_h in acetonitrile at 25–38°C. The value of D_h (28.8 nm) in THF at 25°C is identical to that in acetonitrile. However, the D_h increases rapidly in *m*-xylene

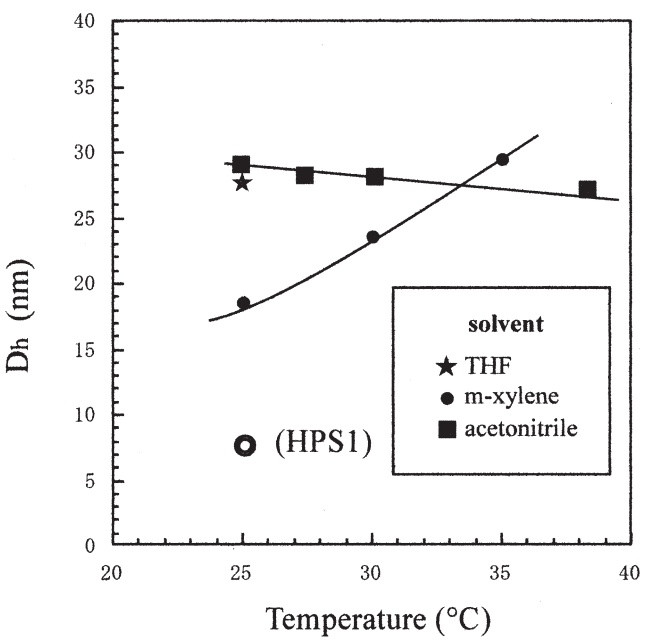

Figure 5 Relationship between hydrodynamic diameter D_h of M-SHPS11 in acetonitrile or *m*-xylene and temperature.

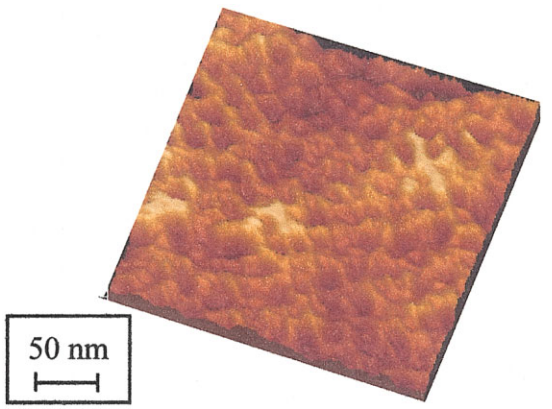

Figure 6 AFM photograph of M-SHPS11 on mica substrate. [Color figure can be viewed in the online issue, which is available at www.interscience.wiley.com.]

with increasing the temperature. At 25°C in *m*-xylene (Θ state), the value of R_g/R_h for M-SHPS11 was 0.73 (R_g = 6.8 and R_h = 9.3 nm). Then M-SHPS11 seems to behave as hard spheres at this temperature, because this condition corresponds to the Θ state. Therefore, the thickness of outer PMMA-grafted chains can be estimated to be ~5 nm in THF or acetonitrile at 25°C. Figure 4(d) shows the SAXS intensity profile of M-SHPS11 in *m*-xylene (25°C) near *C**. Two peaks appear at the relative *q* positions of 1:$\sqrt{4/3}$. In general, the relative *q* positions of 1:$\sqrt{4/3}$ correspond to the packing pattern of (111) and (200) planes in an fcc structure. Therefore, hard nanospheres were packed in the lattice of fcc near *C**. The D_S (22.1 nm) was also identical to D_h (18.6 nm) in *m*-xylene at 25°C.

We also investigated such structural ordering by SAXS measurements at higher concentrations. However, we could not detect strong scattering peaks. To get sufficient signal, it is necessary to secure synchrotron beam time.

AFM characterization

A dilute solution of the synthesized M-SHPS11 copolymer was spin-cast on mica to prepare thin film for AFM studies. Figure 6 shows AFM photograph of M-SHPS11 copolymer. It was found that spherical particles aligned on the mica substrate. The particles ranged over a magnitude of diameter 20–25 nm in a hexagonal array, which agrees with the D_S from the SAXS measurement in *m*-xylene within experimental errors. This means that M-SHPS copolymers may show nano-scaled ordering even in the bulk state. Further work on such ordering is in progress.

CONCLUSIONS

The HPSs were prepared by living radical polymerization of VBDC as an inimer under UV irradiation. Subsequently, we derived SHPS by grafting from HPS macroinitiator with MMA or EMA. It was found from the solution properties that HPS and SHPS behaved in good solvent as hard and soft spheres, respectively. We studied the structural ordering of both branched polymers by means of SAXS measurements. The SHPS copolymers formed a bcc structure in a good solvent near *C**. However, this structure changed to an fcc lattice in the Θ state (*m*-xylene works as Θsolvent for PMMA-grafted chains), because SHPS behaved as hard spheres in such condition. AFM experiments demonstrated that SHPS copolymers aligned with cubic structures on a mica substrate. In the SAXS intensity profile, the HPS showed a single scattering peak in good solvent. The HPS did not take long-range ordering structure, though these nanospheres behaved as a hard sphere.

References

1. Hult, A.; Johansson, M.; Malmstrom, E. Adv Polym Sci 1999, 143, 2.
2. Kim, Y. H. J Polym Sci Polym Chem Ed 1998, 36, 1685.
3. Davis, N.; Rannard, S. Polym Mater Sci Eng 1997, 77, 158.
4. Witten, T. A.; Pincus, P. A.; Cates, M. Europhys Lett 1986, 2, 137.
5. Ishizu, K.; Ono, T.; Uchida, S. J Colloid Interface Sci 1995, 175, 293.
6. Furukawa, T.; Ishizu, K. Macromolecules 2003, 36, 434.
7. Watzlawek, M.; Likos, C. N.; Löwen, H. Phys Rev Lett 1999, 82, 5289.
8. Saito, R.; Kotsubo, H.; Ishizu, K. Polymer 1994, 35, 1580.
9. Ishizu, K. Prog Polym Sci 1998, 23, 1383.
10. Ishizu, K.; Uchida, S. Prog Polym Sci 1999, 24, 1439.
11. Fadeev, M. A.; Rebrov, A. V.; Ozerina, L. A.; Gorbatsevich, O. B.; Ozerin, A. N. Polym Sci 1999, A41, 189.
12. Pötschke, D.; Ballauff, M.; Linder, P.; Fischer, M.; Vögtle, F. Macromolecules 1999, 32, 4079.
13. Nisato, G.; Ivkov, R.; Amis, E. J. Macromolecules 1999, 32, 5895.
14. Topp, A.; Bauer, B. J.; Klimash, J. W.; Spindler, R.; Tomalia, D. A.; Amis, E. J. Macromolecules 1999, 32, 7226.
15. Topp, A.; Bauer, B. J.; Tomalia, D. A.; Amis, E. J. Macromolecules 1999, 32, 7232.
16. Topp, A.; Bauer, B. J.; Prosa, T. J.; Scherrenberg, R.; Amis, E. J. Macromolecules 1999, 32, 8923.
17. Muzafarov, A. M.; Gorbatsevich, O. B.; Rebrov, E. A.; Ignteva, G. M.; Chenskya, V. S. Polym Sci 1993, A35, 1575.
18. Ozerin, A. N.; Sharipov, E. Y.; Ozerina, L. A.; Goluboko, N. V.; Yanovskaya, M. I. Russ J Phys Chem 1999, 73, 221.
19. Ohshima, A.; Konishi, T.; Yamada, J.; Ise, N. J. Phys Rev E: Stat Phys Plasmas Fluids Relat Interdiscip Top 2001, 64, 051808.
20. Ishizu, K.; Mori, A. Macromol Rapid Commun 2000, 21, 665.
21. Ishizu, K.; Shibuya, T.; Mori, A. Polym Int 2002, 52, 424.
22. Moad, G.; Rizzardo, E. Macromolecules 1995, 28, 8722.
23. Ishizu, K.; Ohta, Y.; Kawauchi, S. Macromolecules 2002, 35, 3781.
24. Ishizu, K.; Shibuya, T.; Kawauchi, S. Macromolecules 2003, 36, 3505.
25. Ishizu, K.; Mori, A. Polym Int 2001, 51, 50.
26. Roovers, J.; Martin, J. E. J Polym Sci Polym Phys Ed 1989, 27, 2513.
27. Yamakawa, H. in Modern Theory on Polymer Solution; Harper and Row: New York, 1971; p 321.
28. Antonietti, M.; Bremser, W.; Schmidt, M. Macromolecules 1990, 23, 3796.
29. Quadrat, O.; Bohdanecký, M. J Polym Sci Part A-2: Polym Phys 1967, 5, 1309.